Experimental Demonstration of an Oscillator Stabilized Josephson Flux Qubit

R. H. Koch, G. A. Keefe, F. P. Milliken, J. R. Rozen, C. C. Tsuei, J. R. Kirtley, and D. P. DiVincenzo
IBM Watson Research Center, Yorktown Heights, New York 10598, USA
(Received 2 November 2005; published 27 March 2006)

We experimentally demonstrate the use of a superconducting transmission line, shorted at both ends, to stabilize the operation of a tunable flux qubit. Using harmonic-oscillator stabilization and pulsed dc operation, we have observed Larmor oscillations with a single shot visibility of 90%. In another qubit, the visibility was 60% and there was no measurable visibility reduction after 35 ns.

DOI: 10.1103/PhysRevLett.96.127001 PACS numbers: 85.25.Dq, 03.67.Lx

In the past few years, great progress has been made in improving the performance of all types of Josephson-based qubits. Reported visibility and coherence times have progressed remarkably [1,2], and two-qubit demonstrations have been reported [3]. To achieve further progress towards truly scalable qubits, a promising next step is to couple the qubit to a harmonic oscillator [1]. This strategy is particularly suited to flux qubits, because the coupling strength can be made extremely strong and because the problem of exponential dependence of the qubit eigenfrequency on the control parameters can be circumvented using harmonic-oscillator stabilization [4]. In this Letter, we report an experimental realization of this idea.

Our qubit [4,5] consists of three Josephson junctions, three loops, and a harmonic oscillator as shown in the inset in Fig. 1. The bare qubit has two control parameters [6], the flux Φ and the control flux Φ_c. This allows the qubit to have a tunable difference frequency between the ground and first excited states, f_{01}, and at the same time to be biased at a degenerate point with respect to the flux parameter Φ. This condition can be met for a wide range of junction critical currents. This flexibility of our structure is a very desirable property for a scalable qubit. To stabilize the operation of our qubit and increase its coherence time, we couple the bare qubit to the lowest mode of a superconducting transmission line, which we model as a harmonic oscillator [4].

Figure 1 shows the simulated eigenfrequencies as a function of the control flux for $\Phi = \Phi_0$. Below about $\Phi_c = 0.4\Phi_0$ and, in particular, at the measurement point, the potential has a double-well structure in the space of the three junction phases (see Ref. [5] for a detailed analysis of this potential), and the eigenstates of the qubit are $|\text{left}\rangle$ and $|\text{right}\rangle$. f_{01} is very small through this region (<50 MHz), but its exact value depends on unavoidable experimental asymmetry between the two wells. The lowest resonant frequency of the transmission line was selected to be 1.5 GHz. At the measurement point or "home base," the eigenstates of the qubit and transmission line are product states; i.e., the two subsystems are effectively uncoupled. If the control flux is increased to about $0.41\Phi_0$, the double well changes to a single well, and the nature of the bare qubit eigenstates changes $|\text{left}\rangle$ and $|\text{right}\rangle$ to $|\text{symmetric}\rangle$ and $|\text{antisymmetric}\rangle$. We have called this the "portal region" [4].

In the absence of the transmission line, the value of f_{01} would be exponentially increasing with control flux. However, the presence of the transmission line creates an avoided crossing in the eigenspectrum as shown in Fig. 1. At larger values of control flux near the operating point, the two lowest energy states are simple harmonic-oscillator eigenstates. Superpositions of these states are highly coherent, because the eigenfrequency difference is independent of the exact value of the control parameters or of the critical current of the junctions. The qubit can be "parked" here with minimum decoherence and crosstalk-induced dephasing. The value of Δ at the avoided crossing (Fig. 1) can be made very large using inductive coupling between the bare qubit and the transmission line.

Figure 2(a) plots the simulated supercurrent circulating in the flux loop, and Fig. 2(b) is the corresponding measured plot. Both plots are obtained by fixing the value of the Φ_c and ramping Φ back and forth. As discussed elsewhere [5], the observation of hysteresis in these plots reflects the existence of a double-well potential. Along the "symmetric line" or "S line," the double well is symmetric, so $\partial f_{01}/\partial\Phi = 0$ (this is referred to as the

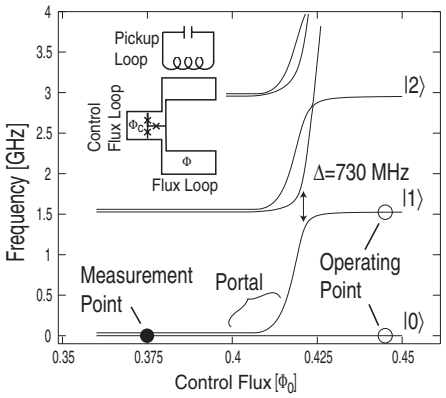

FIG. 1. The simulated eigenfrequency vs control flux for qubit A, described below, for $\Phi = \Phi_0$. The inset is a schematic representation of the bare qubit coupled to a harmonic oscillator. The mutual inductance (M in Fig. 3) between the bare qubit and the transmission line is 200 pH.

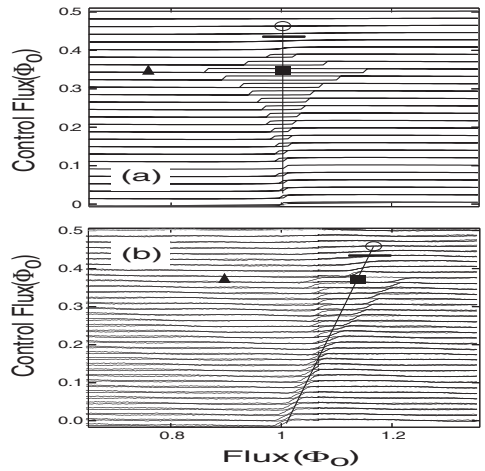

FIG. 2. (a) Simulated current in the pickup loop vs flux Φ, parametrized by the control flux Φ_c. (b) The corresponding experimental data, measured for our qubit A (described below) at a flux sweep frequency of 13 Hz. The square symbol marks the measurement point, the open dot the operating point, and the triangle the reset point. The solid vertical line is the ''S line'' or symmetric-well line. The solid horizontal line near the operating point represents the range of flux biases used to collect the data shown in Fig. 4(b). The measured hysteresis is smaller than the simulated because the simulation does not include thermal or quantum fluctuations. The tilting of the measured data is a result of inadvertent mutual inductance between the control-flux drive loop and the flux loop. The hysteresis seen in the experimental data near $\Phi = 0.7\Phi_0$ is hysteresis of the measurement circuit and not of the qubit.

''degeneracy condition'' with respect to Φ). If Φ is decreased (or increased) from the S-line value, the well is tilted so that the left (or right) well has a lower energy. Far from the S line, the double well becomes a single well and the hysteresis vanishes. This property allows the qubit to be prepared in either the left or right eigenstates by simply applying flux pulses. To operate the qubit, we dc bias the qubit at the measurement point, and we apply a control-flux pulse to bring the qubit to the operating point. In these devices, we also apply a simultaneous flux pulse to compensate for the tilting of the experimental curves. For small amplitude control-flux pulses, the amplitude determines the f_{01}. Usually, we adjust the amplitude to be well beyond the avoided crossing in Fig. 1; in this case, f_{01} is simply the resonator frequency. At the measurement point, a dc SQUID is used to measure the circulating current in the pickup loop so the state of the qubit can be determined.

The operation of our qubit involves only simple pulses (as in, e.g., Ref. [7]); microwave excitation is not used. We set the qubit in the $|0\rangle$ state at the measurement point, rapidly pulse the qubit to the operating point, hold it there, pulse it back, and measure the final state of the qubit. By varying the amount of time at the operating point, we observe Larmor oscillations of the final state of the qubit between the $|0\rangle$ and $|1\rangle$ states. At the measurement point, the transition rate between the two ''deep'' wells is exponentially small; i.e., the qubit is frozen in the left or the right state. The measured T_1 time is 5 ms or longer even when operating at a noise temperature of 60 K on the flux and control-flux lines. We note that the reset pulse sequence adiabatically cools the qubit.

A slow adiabatic control-flux pulse from the measurement point to the operating point will not create a linear superposition between the $|0\rangle$ and $|1\rangle$ eigenstates needed to demonstrate Larmor oscillations in our qubit. The pulse must have a fast enough rise time when passing through the portal region so that the evolution there is not adiabatic. For example, if the qubit is initially set in the left or $|0\rangle$ state and adiabatically (slowly) pulsed through the portal region, the qubit will remain in the $|0\rangle$ state even as this state becomes the symmetric ground state. The wave function amplitude will smoothly go from being all on the left side of the potential to being symmetrically in both potential wells. This evolution takes time and depends on the effective mass. If the pulse rise time is fast enough and the junction capacitance or effective mass is large enough, the wave function will not have time to evolve out of the left well, and the quantum system, after being pulsed though the portal, will be in a linear combination of the symmetric state $|0\rangle$ and the first excited state $|1\rangle$ (since this superposition state is confined to the left side of the potential). Thus, an equal superposition of $|0\rangle$ and $|1\rangle$ is created [4].

The control-flux pulse takes the system from the measurement point to the operating point. While the pulse must rise rapidly through the portal, the rise time must be slow enough to avoid excessive Zener tunneling near the avoided crossing. Hence, we optimize our qubits to have a large gap Δ. We can estimate the gap by measuring the mutual inductance between the bare qubit and the transmission line using the readout SQUID and then computing the eigenspectrum using the measured parameter from the plot in Fig. 2(b). We simulate the dynamics resulting from the control-flux pulse using a numerical, time-dependent solution of the Schrödinger equation; see [4,5]. We find that for our parameters, a transit time of 0.4 ns though the portal will create the required superposition state and avoid excessive Zener tunneling. Our pulsing system only has a rise time of 0.6 ns, but we create an effectively faster rise time by increasing the amplitude of the control-flux pulse by moving the operating point from about $\Phi_c = 0.45$ to $0.60\Phi_0$. Because the bands are flat at large Φ_c in Fig. 1, ''overshooting'' the operating point has no detrimental effects.

Figure 3 describes the experimental setup we use to operate our qubits. The dc current needed to flux bias the qubit is provided by a battery, an ultrastable voltage regulator, ultralow temperature coefficient of resistance resistors, and two stepper-motor-controlled potentiometers for coarse and fine adjustment. The dc currents bias the qubit at the measurement point (the square in Fig. 2). The pulses needed to operate the qubit are provided by a combination of a Tektronix AWG430 arbitrary waveform generator, which supplies the reset pulse (the triangle in Fig. 2), and

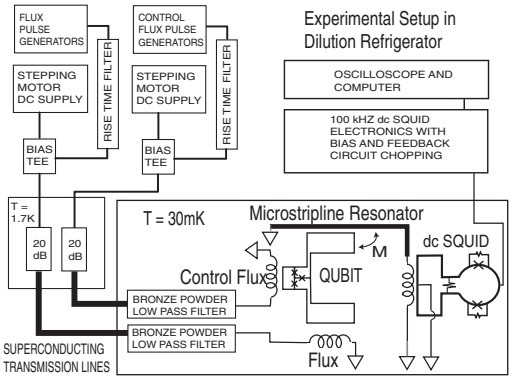

FIG. 3. Schematic of the experimental setup.

a Tektronix DTGM30 pulse generator, which supplies the operating pulse (the open dot in Fig. 2). We use a 1 μs reset pulse. The bare rise time of the pulse generator is less than 0.1 ns. Each source can be independently rise-time filtered and the outputs can be summed together. We use a room temperature bias tee. There is an identical circuit for the control flux.

We filter each signal to the qubit with a low-pass filter made using bronze powder and epoxy, packed around a single straight superconducting wire [8]. These filters have a characteristic impedance of 50 Ω and an attenuation of -20 dB at 1.5 GHz, which limits the (measured) rise time of the pulse to 0.6 ns. The dc noise temperature of the flux-bias circuits, without the pulse generators, is 4.7 K. The two pulse generators have output noise temperatures from 500 000 to 1 000 000 K, depending on their settings. By using attenuators on their outputs, the dc noise level from the generators at the qubit can be reduced, varying from 60 to 3 K. The bronze-powder filters attenuate the dc noise so that, at the qubit operating frequency of $f_{01} = 1.5$ GHz, the effective noise temperature is between 0.047 and 0.6 K, depending on the pulse attenuators that are used. The entire pulse launching circuit is designed to have a 50 Ω characteristic impedance. The largest measured impedance error was 4 Ω.

The bare qubit is fabricated using Al stripes, Al oxide junctions, and shadow deposition [9]. Most of the data reported here are measured using junctions that are 300 by 300 nm in size and having a thermodynamic critical current of 0.55 to 0.60 μA. The capacitance was estimated to be 20 fF, including stray capacitance. The self-inductance of the small loop of the qubit is 30 pH, and each of the large loops has a self-inductance of 600 pH. The bare qubit is flux and control-flux biased using microstrip transmission lines. The lines are 50 μm wide patterned on a 60 μm thick silicon wafer. At the bottom of the wafer is a niobium ground plane. The mutual inductance between the control lines and the qubit loops are both 0.5 pH. The bare qubit is inductively coupled to a niobium microstrip transmission line. The line is directly shorted at one end and shorted at the other end by the input loop of a dc SQUID. Using the measured phase velocity of the line and the self-inductance of the dc SQUID and the interconnecting wire bonds, we can predict the frequency of the lowest mode of the transmission line resonator. The error between the prediction and the measured value is very small, about 80 MHz.

The readout SQUID was either an IBM or a Hypres thin film dc SQUID. The SQUID is operated by ordinary an 100 kHz feedback loop that was modified to have better stability and lower noise. The SQUID is operated in a chopped mode. During the control-flux pulse, the SQUID is blanked; i.e., the bias current and feedback and modulation fluxes are zeroed. The qubit and SQUID were enclosed in a superconducting box.

The measurement sequence has six steps: (1) apply the reset pulse, (2) verify the state of the qubit (this is not really necessary), (3) blank the SQUID, (4) apply the control-flux pulse, (5) unblank the SQUID, and (6) measure the final state of the qubit. The coupling between the SQUID and the qubit is such that, given the SQUID noise level, we can determine the state of the qubit in 100 μs with essentially no errors introduced by SQUID noise. This sequence is repeated 300 times per second (the repetition rate could be made much faster). Since the qubit has a huge barrier between the left and right energy wells at the measurement point, the noise associated with the SQUID measurement and the blanking and unblanking of the SQUID do not switch the state between left and right. After blanking the SQUID, we wait 20 μs to allow the qubit to relax into the ground state of the well in which it lies.

Figure 4 summarizes the results of measurement on two qubits, referred to here as A and B. Our best measured visibility, on qubit A, is 90% as shown in Fig. 4(a). Here we are, as discussed earlier, pulsing the control flux to beyond the operating point in Figs. 1 and 2 to compensate for our experimental rise time of 0.6 ns. The visibility is limited by the speed of passage through the portal region and also by imperfections in setting Φ to its S-line value of Φ_0. We find that increasing the rise time of the control-flux pulse from 0.6 to 2 ns reduces the measured visibility to 4%. Qubit A has a particularly large visibility because the gap in the energy spectrum at the avoided crossing is, according to modeling, 730 MHz. In another device identical to qubit A, except that the mutual inductance (measured) and energy gap (inferred) is 4 times smaller, no signal is seen because the Zener tunneling rate was too high.

Figure 4(b) demonstrates how changing the final flux value away from the optimal value of $1.0\Phi_0$ tilts the potential left or right and changes the final switching probability for qubit A. Each of the curves starts from the same measurement point and involves pulsing the control flux to the same value, but the value of the flux at the operating point is varied over the range indicated in Fig. 2. The middle curve on the seven curves in this panel is for $\Phi = \Phi_0$. For a more negative (or positive) pulsed flux, the potential is tilted left (or right), and the mean probability of switching is closer to 0 (or 1).

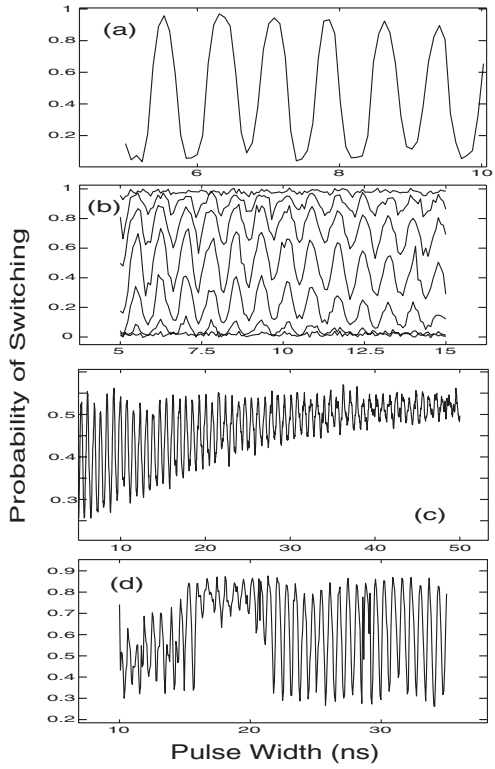

FIG. 4. (a)–(c) Results for qubit A. (a) The probability of switching from the initial starting well (left) to the other well (right) after application of a control-flux pulse vs pulse duration for $\Phi_c = 0.6\Phi_0$. Each data point represents the average of 460 single shot measurements. (b) The probability of switching vs pulse duration for seven uniformly spaced values of flux ($\pm 0.035\Phi_0$) at $\Phi_c = 0.43\Phi_0$, as depicted by the horizontal lines of length $0.07\Phi_0$ in Fig. 2. (c) shows the probability of switching as the pulse duration is made longer. The observed Larmor oscillation frequency of the upper three panels is 1.28 GHz. (d) plots the Larmor oscillations of qubit B using only the arbitrary waveform generator as a pulse source. The oscillation frequency is 1.44 GHz and the coherence time is substantially longer than 35 ns. The poorly defined behavior below 16 ns and the gap in the oscillations from 16 to 21 ns result from pulse distortions produced by the arbitrary waveform generator. When the pulse length is less than a few times the inverse of the maximum clock frequency (200 MHz), the resulting pulse waveform is severely distorted.

Figure 4(c) plots the decay of the Larmor oscillations with time for qubit A. The coherence time is limited by the loop shunt resistor of the readout SQUID. This resistor is not in parallel with a SQUID Josephson junction but in parallel with the SQUID loop inductor; see Fig. 3. Using measured values, the Q of the transmission line is predicted to be 28, implying a predicted energy relaxation time of 23 ns. The measured time is approximately 25 ns, in good agreement with our estimate. The loop shunt resistor is usually added to a SQUID to suppress resonances in multiturn input loops but is really not needed in this situation.

If we remove the loop shunt resistor, or more weakly couple the readout SQUID to the qubit, the coherence time increases dramatically. Figure 4(d) shows data for qubit B, which is one that is coupled more weakly to a different readout SQUID whose loop shunt resistor has a significantly larger resistance. At 35 ns, there is no measurable decay of the Larmor oscillations. Qubit B has a problem with reflections from the dc block, which abruptly terminates the Larmor oscillations at 50 ns. But we can estimate the energy relaxation time to be greater than 300 ns, limited by the SQUID junction shunt. While using a shunted dc SQUID as a readout device is very convenient, achieving coherence times much longer than 1 μs will be very difficult, and a more conventional unshunted SQUID readout scheme [2] will probably be required in future experiments.

In conclusion, our work provides new evidence that harmonic-oscillator modes embodied by transmission lines will be superior carriers of quantum information. Our system has several unique features that offer good prospects for scalability, compared with other Josephson qubits: The transmission line frequency, depending only on one geometric parameter, the length, can be fixed with very high precision. Its insensitivity to the magnetic flux environment when parked on the transmission line will greatly diminish the degree of unintended couplings between qubits. The gradiometric design of the qubit can be exploited to further reduce cross talk during gate operations, when the qubit is moved off the operating point of Fig. 1. These issues of scalability are the most important ones to be explored in the next round of experiments on this qubit system.

We thank Fred Brito, John Bulzacchelli, John Clarke, Abe Elfadel, and Christian Schuster for useful discussions. We thank DARPA for financial support. D. P. D. V. is supported in part by the NSA and ARDA through ARO Contract No. W911NF-04-C-0098.

[1] A. Walraff *et al.*, Nature (London) **431**, 162 (2004).
[2] P. Bertet *et al.*, Phys. Rev. Lett. **95**, 257002 (2005); Yu. Pashkin *et al.*, Nature (London) **421**, 823 (2003); T. Yamamoto *et al.*, Nature (London) **425**, 941 (2003); A. J. Berkley *et al.*, Science **300**, 1548 (2003); A. Izmalkov *et al.*, Phys. Rev. Lett. **93**, 037003 (2004); J. B. Majer *et al.*, Phys. Rev. Lett. **94**, 090501 (2005).
[3] R. McDermott *et al.*, Science **307**, 1299 (2005).
[4] R. H. Koch *et al.*, Phys. Rev. B **72**, 092512 (2005).
[5] D. P. DiVincenzo, F. Brito, and R. H. Koch, cond-mat/0510843.
[6] The flux in the third or pickup loop cannot be independently adjusted when the metal strip around the whole bare qubit is superconducting.
[7] Y. Nakamura, Yu. A. Pashkin, and J. S. Tsai, Nature (London) **398**, 786 (1999).
[8] F. P. Milliken, J. R. Rozen, G. A. Keefe, and R. H. Koch (unpublished).
[9] T. L. Robertson *et al.*, Phys. Rev. B **72**, 024513 (2005).